Tectonophysics 485 (2010) 78–84

Contents lists available at ScienceDirect

Tectonophysics

journal homepage: www.elsevier.com/locate/tecto

Development of the Eastern California Shear Zone — Walker Lane belt: The effects of microplate motion and pre-existing weakness in the Basin and Range

C. Plattner [a,*,1], R. Malservisi [a,2], K.P. Furlong [b,3], R. Govers [c,4]

[a] Ludwig Maximilians Universität München, Dept. of Earth and Environmental Sciences, Germany
[b] Penn State University, Dept. of Geosciences, PA, USA
[c] Utrecht University, Department of Earth Sciences, Netherlands

ARTICLE INFO

Article history:
Received 7 May 2009
Received in revised form 24 November 2009
Accepted 25 November 2009
Available online 2 December 2009

Keywords:
Western North America
Sierra Nevada
Baja California
Mojave block
Numerical modeling

ABSTRACT

The role that the motion of microplates has played in the development of the Eastern California Shear Zone in western North America is unclear. It was previously proposed that shear related to Baja California motion has propagated from the Gulf of California northward into Nevada. However, there is evidence that the formation of the Eastern California Shear Zone predates the inception of Baja California motion. Thus, either Baja California began to move northwestward prior to 6 Ma, or the Eastern California Shear Zone formed by shear strain resulting from different microplate motion than Baja California. The role of Sierra Nevada motion on the development of an adjacent shear zone remains untested. We present a numerical modeling study that examines the deformational response of western North America to Baja California and/or Sierra Nevada microplate motion. In particular we study if, and under what condition of microplate motion, shear strain can localize in the northern and southern part of the Eastern California Shear Zone (separated by the Garlock fault). We find that given the pre-existing weakness from Miocene Basin and Range extension (a lithospheric strength contrast or normal faults) shear strain from either the Baja California or Sierra Nevada microplates can lead to the formation of the Eastern California Shear Zone. Furthermore, the presence of a pre-existing weakness explains the earlier initiation of strike-slip faulting north of the Garlock fault. Our models suggest that today, Baja California microplate motion is the major player for present-day deformation rates along the Eastern California Shear Zone and was in the past 6 Myrs also a major driver of strain localization in southern Eastern California Shear Zone within the Mojave block.

1. Introduction

Western North America straddles a complicated and diffuse plate boundary between the North America (NAM) and Pacific (PAC) plates. Within this diffuse plate boundary, deformation concentrates along narrow shear regions separated by tectonically rigid blocks (here also called microplates). Although most of the relative displacement between NAM and PAC is accommodated along the San Andreas Fault system (SAF), approximately 25% of the deformation is located along the Eastern California Shear Zone (ECSZ) (Dixon et al., 2000a; Miller et al., 2001). This strike-slip zone is bounded on the east by diffuse extensional deformation (Basin and Range) and the undeformed tectonic block of Sierra Nevada on the west (SIERRA microplate) (Fig. 1). How this intra-continental plate boundary developed and what role surrounding rigid blocks and weak extensional regions play in its formation are still open questions. It has been suggested (Faulds et al., 2005a,b; Harry, 2005; McCrory et al., 2009) that the ECSZ formed by northward propagation of the plate boundary in the Gulf of California due to the northward motion of the Baja California peninsula (BAJA microplate). Translation of BAJA with the Pacific plate began around 6 Ma when the plate boundary had fully migrated westward and formed the Gulf of California transtensional fault system (Lonsdale, 1991; Atwater and Stock, 1998). Prior, between 12 and 6 Ma the so-called Protogulf hosted east–west extension, and shear was accommodated west of BAJA (Stock and Hodges, 1989). Geological studies have dated initiation of strike-slip faulting in the ECSZ to 12–10 Ma (Reheis and Sawyer, 1997; McQuarrie and Wernicke, 2005), with single faults exhibiting dextral slip as early as 19 Ma (Bartley et al., 1990). This implies that there was either older northerly displacement of BAJA (Fletcher et al., 2007) or an alternate earlier driver for shear strain localization in western NAM. Several observations suggest the need for alternative mechanisms for the formation of the

* Corresponding author. Fax: +49 8921804205.
E-mail addresses: plattner@geophysik.uni-muenchen.de, cplattner@rsmas.miami.edu (C. Plattner), rocco@cas.usf.edu (R. Malservisi), kevin@geodyn.psu.edu (K.P. Furlong), govers@geo.uu.nl (R. Govers).
[1] Present address: University of Miami, Rosenstiel School of Marine and Atmospheric Sciences, Marine Geology and Geophysics, Miami, FL 33149, USA. Fax: +1 3054214632.
[2] Present address: University of South Florida, Dept. of Geology, Tampa, FL 33620, USA.
[3] Fax: +1 814 8637828.
[4] Fax: +31 302535030.

0040-1951/$ – see front matter © 2009 Elsevier B.V. All rights reserved.
doi:10.1016/j.tecto.2009.11.021

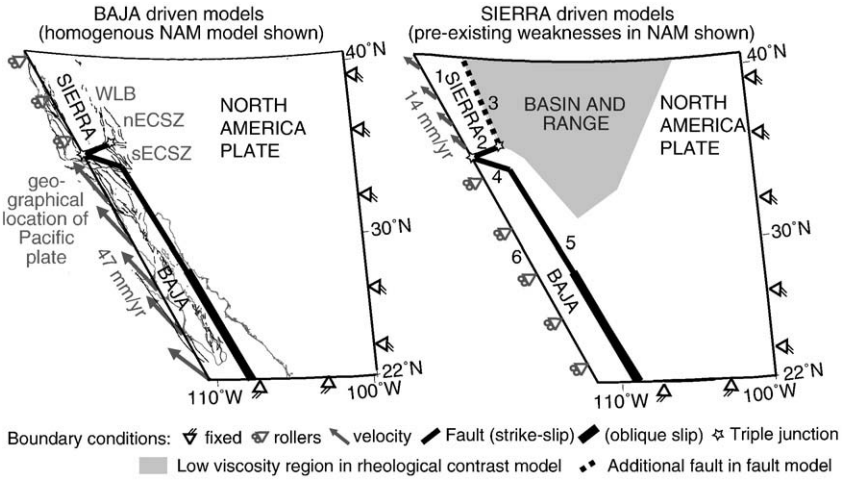

Fig. 1. Left panel shows model geometry and boundary conditions for the BAJA driven model with homogenous NAM. Right side shows the model setup for SIERRA driven models, and model alterations for simulating pre-existing weaknesses in NAM: gray shaded area shows region where viscosity was lowered from 10^{23} Pa s to 10^{21} Pa s, dashed line indicated added strike-slip fault along the ECSZ–WLB. "Rollers" allow nodal displacement along-strike the model boundary. Model domain boundaries, model faults: (1) San Andreas Fault (SAF), (2) Garlock Fault, (3) nECSZ–WLB, (4) SAF restraining bend, (5) BAJA–NAM plate boundary (Gulf of California), and (6) PAC–BAJA plate boundary. The Mojave block is located between 3, 4, and 6.

ECSZ than northward propagation of shear from the Gulf of California. There is no observed connection across the Garlock fault between the southern and northern part of the ECSZ (Dokka and Travis, 1990). The northern part of the ECSZ (nECSZ) comprises the Owens Valley Fault Zone, Panamint Valley — Hunter Mountain Fault Zone, Death Valley — Fish Lake Valley Fault Zone. We include also the Walker Lane belt fault zone. The southern part of the ECSZ (sECSZ) is located within and adjacent to the Mojave block, As much as 90% of the faulting in the southern part (often referred to as the Mojave Shear Zone, here called sECSZ) occurred only after 4 Ma (Miller and Yount, 2002; Oskin and Iriondo, 2004). Thus, geological observations suggest that the sECSZ initiated after the northern ECSZ had already experienced significant shear.

Plattner et al. (2009) showed that at present, rigid block motion of SIERRA can be driven by BAJA motion which in turn is driven by partial coupling to PAC. However, the tectonic history of both microplates makes it likely that in the past lateral drag resulting from coupling with the PAC motion also acted directly on the western margin of SIERRA (Nicholson et al., 1994). SIERRA microplate motion could have been driven by this mechanism since 15–20 Ma, and could have lead to the formation of the nECSZ prior to the development of the plate boundary within the Gulf of California and the beginning of BAJA northward migration. To test this hypothesis we use finite element models to examine the shear deformation associated with SIERRA and BAJA microplate motion. In particular, we want to assess i) if, and under what conditions, lateral tractions applied to SIERRA can lead to shear zone formation in western NAM (representing the situation ~12 Ma), ii) if, and under what conditions BAJA motion can drive shear zone formation in the nECSZ prior to the formation of the sECSZ (representing the period between 12 and 4 Ma, assuming earlier northerly transport of BAJA), and iii) how the formation of the sECSZ may have been influenced by an earlier formation of the nECSZ (at any time of nECSZ formation prior to 4 Ma). We also assess the role of lateral strength variations between the western NAM and the extended and weak Basin and Range Province, and of pre-existing regional fault zones.

2. Model description

To address these questions, we test two end-member deformation models driven by the motion of either the BAJA microplate or by SIERRA microplate, i.e., one of the microplates is driven by kinematic boundary conditions while the other microplate and NAM respond in a passive way. In both cases we test the deformational response in western NAM, assessing whether that model enhances the development of a shear zone along the nECSZ, along the sECSZ, or neither. We also test the effect of lateral variations in lithosphere strength on the development of a shear zone between the SIERRA and the Basin and Range. Finally, we test the influence of the reactivation of Basin and Range normal faults as shear zones by assuming pre-existing faults east of SIERRA.

For the numerical modeling we use the finite element code GTECTON with 2D plane stress spherical thin shell elements (Govers and Meijer, 2001). GTECTON solves the mechanical equilibrium equations and computes the deformation resulting from our boundary conditions and model geometries.

The model domain (Fig. 1) is a three-plate configuration, including the North America plate, and the BAJA and SIERRA microplates. The western edge of the domain is taken along the SIERRA–PAC and BAJA–PAC microplate boundaries, where interaction of these microplates with the PAC is represented by kinematic boundary conditions (velocities). The plate boundaries (faults) follow the main fault-trace (Meade, 2007) adapted to represent the plate configurations ~12–6 Ma. Assuming translation of BAJA with the PAC plate during this time implies accommodation of shear in the Protogulf, and transpression north of BAJA. Thus, in these models we separate BAJA from the NAM plate by a weak shear zone, represented by faults. For better comparison of the model results, we use the same representation of the Protogulf and SAF restraining bend also in the SIERRA driven models. We discuss the relevance of this assumption for both end-member models later. The southern end of the SIERRA block is bounded by the Garlock fault already active in the time frame of interest (Monastero et al., 1997). The model does not include the sECSZ since we are studying the conditions that lead to its development. We also test different assumptions for the nECSZ (as explained below).

All model plate boundaries and faults (same representation) are vertical and frictionless, allowing strike-slip in response to shear stresses on the model fault (Melosh and Williams, 1989). Protogulf extension is modeled by allowing both strike-slip and normal relative motion south of 27°N, as this best represents BAJA kinematics (Plattner et al., 2009). Fault intersections are modeled by triple overlapping nodes.

Velocity boundary conditions are specified w.r.t. stable NAM. Therefore, eastern and southern boundaries of the NAM part of the model domain are fixed. The northern boundary of NAM is free to move north. We choose this assumption because, as we analyze shear

strain pattern, we prefer to under- rather than overestimate resistance to motion of SIERRA and BAJA. The influence of this boundary condition on the model results will be discussed later. The imposed velocities are equal to the relative rigid plate motion of the driving microplate with respect to stable NAM. The BAJA–NAM motion is derived from Plattner et al. (2007) with an approximate rate of 47 mm/year and azimuth of N50°W, while SIERRA–NAM motion is derived from Psencik et al. (2006) (14 mm/year to N55W°). These velocity boundary conditions represent a measure of mechanical coupling between the respective microplate and the PAC plate (Plattner et al., 2009). Thus the magnitude of the boundary condition equals the full PAC–NAM rate minus the long-term amount of slip accommodated at the corresponding boundary. Later we discuss the influence of the use of present-day rigid plate velocity boundary conditions in a model representing the period between 12 and 6 Ma.

In our 2D spherical shell models, we use an elastic-viscous rheology to represent the (vertically averaged) lithospheric mechanical properties. We use an average viscosity of 10^{23} Pa s compatible with a powerlaw rheology for continental lithosphere with a 60 mW/m^2 surface heat flow, a 30 km thick granitic crust overlying a 70 km thick dry olivine lithospheric mantle, and a strain rate of 10^{-15} s^{-1} (Ranalli, 1995). In the first sets of models the average viscosity is applied to the entire model domain. We also test a weakened Basin and Range (Fig. 1) to investigate the effect of rheological contrast on the development of the ECSZ; the average viscosity in the Basin and Range is set to a lower regional average value of 10^{21} Pa s (Flesch et al., 2000; Malservisi et al., 2001), which is consistent with higher heat flow in an extensional regime (Lachenbruch and Sass, 1978) (90 mW/m^2 steady state surface heat flow, 20 km thick granite crust overlying a 80 km thick lithospheric mantle). We also analyze the role in the development of the ECSZ as reactivation of normal faults along the western border of the Basin and Range by including a pre-existing fault, which can move by strike-slip. These models have homogenous rheology. Concerning the density of the finite element mesh, we verified that all our models have converged by demonstrating the insensitivity of the results to changes in the element size.

3. Modeling results

Model results in map view show the maximum shear strain rate from the local strain tensor (Fig. 2). The direction of this maximum shear strain is not necessarily oriented parallel to plate motion. Fig. 3 shows two profiles oriented perpendicular to the plate motion direction, where shear strain is calculated from the plate motion parallel velocity. Note that it is likely, that the strain magnitude in Fig. 3 is lower than from the maximum shear strain. The northern profile (A–A′) crosses the nECSZ at the approximate location of the 1872 Owens Valley earthquake (Beanland and Clark, 1982), and the southern profile (B–B′) crosses the sECSZ at the approximate location of the 1999 Hector Mine earthquake (Sandwell et al., 2000) (Fig. 2). We expect that localized shear zones from most likely in regions where the shear strain rate is high within a narrow zone.

3.1. Response to BAJA motion

As expected with our model geometry, low strain rates in BAJA (Fig. 2) demonstrate that most of this microplate moves as a rigid block with fault slip along the Protogulf. Northwestward motion of BAJA is hindered at the SAF restraining bend, causing deformation in and around this collision zone. Shear strain is high at the corners of the

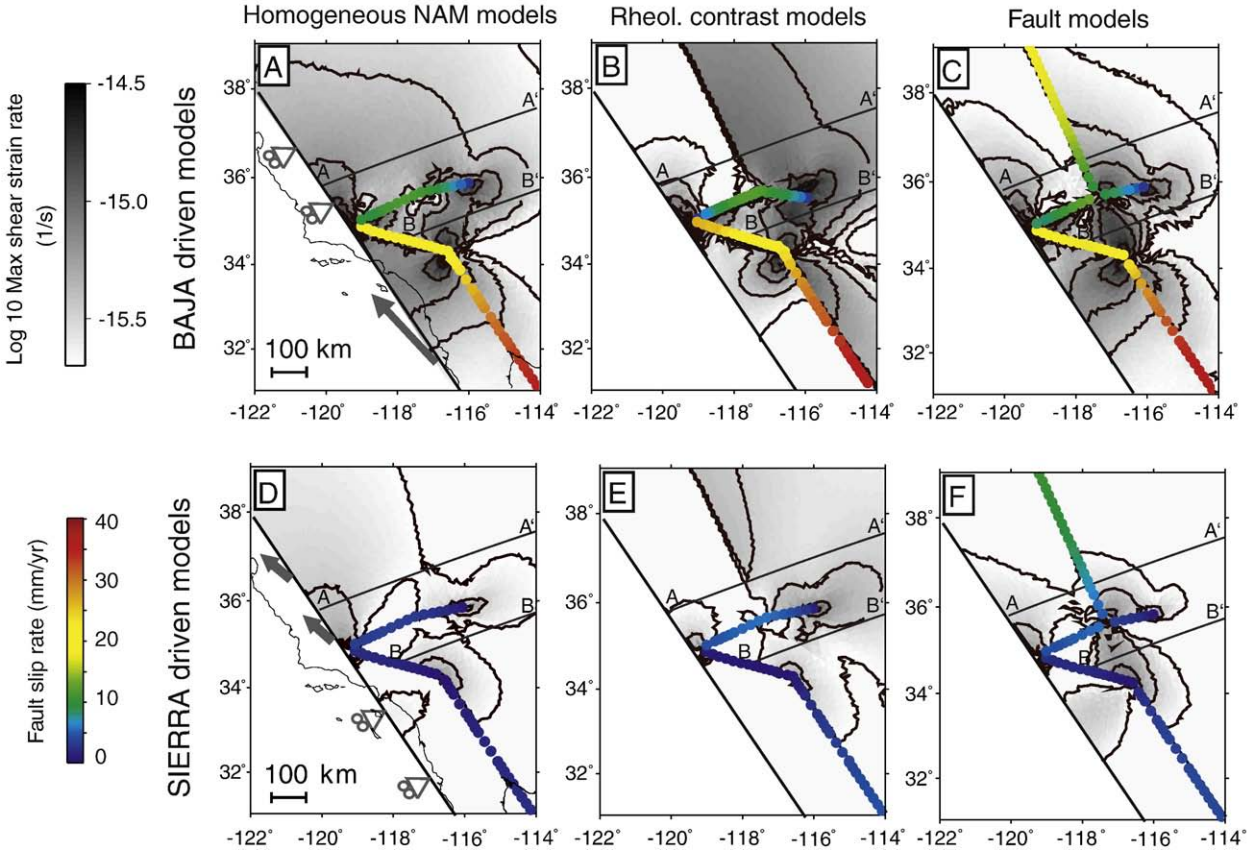

Fig. 2. Pattern of maximum shear strain rate (logarithmic color scale and contour lines) in southwestern North America (NAM) as a response to BAJA motion (upper images) respectively, SIERRA motion (lower images), and in dependency of the strength in western NAM (see column headers). Maximum shear strain derived from constant strain element information (does not show strain localized by fault slip on between elements). Faults are shown color-coded by the slip rate (fault slip rate is not shown at triple junctions). Profiles A–A′ and B–B′ are shown in Fig. 3.

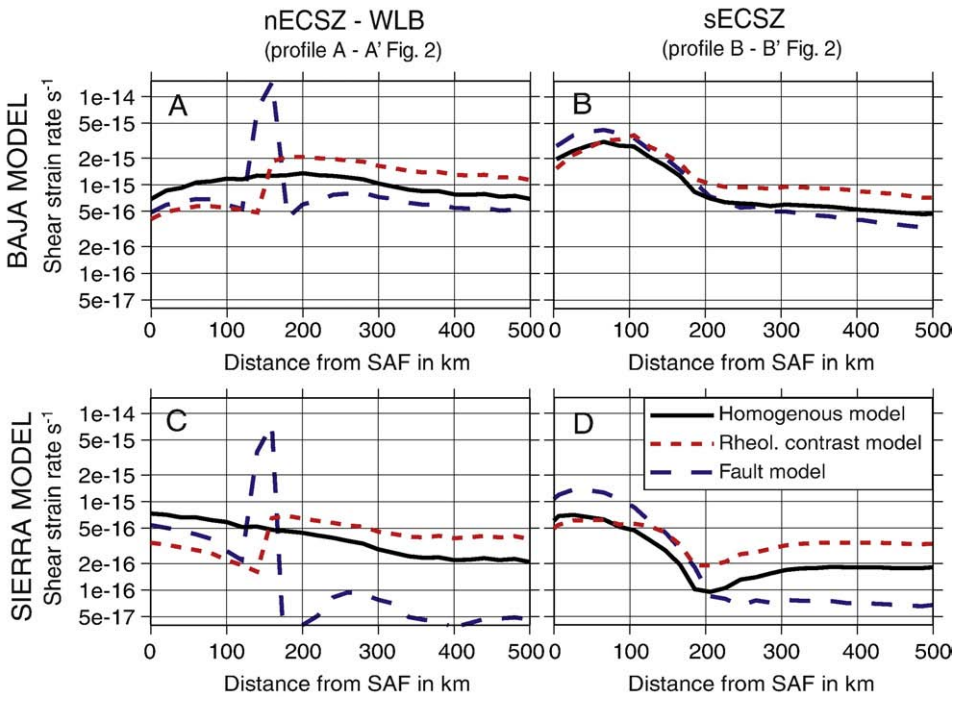

Fig. 3. Shear strain rate with respect to distance from San Andreas Fault (SAF) along the cross-sections A–A′ crossing the nECSZ–WLB and B–B′ crossing the sECSZ (for location of profiles see Fig. 2). With respect to Fig. 2, values are not maximum shear strain rate, but calculated from the derivate of the plate motion parallel velocity. Upper panel shows results from models driven by BAJA motion, lower panel by SIERRA motion. BAJA motion causes larger shear strain rate in the region of the sECSZ. From both microplate motions shear zones along the nECSZ–WLB can form in case of pre-existing weakness in western North America, such as lower viscosity in the Basin and Range area (rheol. contrast model) or fault zones in the Basin and Range (fault model — note that fault slip is equivalent to high strain). Without such weakness (homogenous model) the deformation is broadly distributed over western NAM.

restraining bend and at the eastern end of the Garlock fault. We will see below that in all models dextral fault slip rates on the Protogulf model fault range from 4 cm/year in the south to 2 cm/year in the north. Sinistral fault slip rates on the Garlock Fault range from 0 to 1 cm/year.

3.1.1. Homogenous NAM

Along profile A–A′, (dextral) shear strain rates are almost constant indicating diffuse deformation (Fig. 3A). Along profile B–B′ there are high shear strain rates up to a distance of 200 km from the SAF restraining bend (Fig. 3B), with a maximum at about 80 km from the SAF. This distance corresponds to the present-day location of the sECSZ. This zone with high shear strain trends northeast (Fig. 2A), connecting the corner in the Protogulf — SAF fault with the end of the Garlock fault.

3.1.2. Pre-existing weakness in western NAM

The model with a strength difference between the Basin and Range Province and SIERRA (Fig. 1) shows high total shear strains in the low viscosity region, in particular along the strength contrast (Basin and Range–SIERRA boundary) (Fig. 2B). Shear strain rates are also high in areas between the Gulf of California and the western Basin and Range. Low shear strain rates are found within BAJA and SIERRA, indicating that for this model the two microplates behave as rigid blocks. Along profile A–A′, the rheological contrast at 150 km distance from the SAF produces a sharp increase in the shear strain rate from low rates at SIERRA to high rates in the Basin and Range (Fig. 3A). The shear strain reaches its maximum. Along profile B–B′ shear strain localizes again in the sECSZ but with higher rates and slower decay east of it (Fig. 3B).

3.1.3. Pre-existing faults in western NAM

We also test the effect on the deformation pattern of the existence of a fault zone (irrespective of a strength contrast between the Basin and Range and SIERRA) that was inherited from Basin and Range extension. The model fault along the nECSZ is activated as a right-lateral strike-slip fault with slip rates of 10–20 mm/year (Fig. 2C). Strike-slip on the fault reduces the shear strain in the Basin and Range with respect to the rheology contrast model. In SIERRA, shear strain rates are only slightly higher than in the rheological contrast model indicating that in this case also SIERRA is moving as a quasi-rigid block. In profile A–A′, relative displacement along the fault appears as a shear strain peak at distance 150 km from the SAF, with distinctly lower strain rates in the SIERRA and the Basin and Range (Fig. 3A). A NNW trending shear zone connects the Protogulf — SAF kink with the end of the nECSZ fault. In profile B–B′, this shows as a maximum shear strain rate at 70 km distance from the NAF.

3.2. Response to SIERRA motion

The second end-member model considers the response of the region to the application of transtensional velocity boundary conditions (~14 mm/year) along the western SIERRA boundary. The SIERRA motion mainly affects regions east of the SAF, SIERRA and Basin and Range, where the deformational response in western NAM depends strongly on the presence of pre-existing weakness. Strain rates in the south, in BAJA and around the SAF restraining bend are lower. For all the models, slip rates on both the Garlock Fault and on the Protogulf are very close to zero (implying that the presence of the Protogulf Fault is not essential for the SIERRA driven model results).

3.2.1. Homogenous NAM

Shear strain rates are highest in SIERRA, directly east of the SAF (Fig. 2D). Along the profile A–A′, the shear strain gradually decreases with distance from the SAF without any apparent regional strain concentration (Fig. 3C). South of the Garlock fault, the shear strain is highest near the corner in the restraining bend of ProtoGulf–SAF system, and at the eastern end of the Garlock fault. There is no through going shear zone observable in the region of the sECSZ.

3.2.2. Pre-existing weakness in western NAM

In the model with a viscosity contrast between the Basin and Range Province and SIERRA, the shear strain is higher in the low viscosity zone. Low strain rates within SIERRA indicates rigid block motion (Fig. 2E), except near the intersection of Garlock fault and the SAF. Along profile A–A′, the rheological contrast at 150 km distance from SAF is evident by the sharp increase in the shear strain rate from low rates at SIERRA to high rates in the Basin and Range (Fig. 3C). Within the Basin and Range there is high shear strain near the rheological contact with rates decaying slowly to the east (Fig. 3C). Along profile B–B′, a broadly deforming area is found around the SAF restraining bend corner and in the Basin and Range, with lower rates in between (Fig. 3D).

3.2.3. Pre-existing fault in western NAM

Up to 12 mm/year of differential motion between SIERRA and the Basin and Range occurs on the pre-existing fault (Fig. 2F). Along profile A–A′, the shear strain rate peaks at the fault at a distance of 150 km from the SAF (Fig. 3C). While some shear strain remains within the SIERRA, the Basin and Range has shear strain rates close to zero. South of the Garlock fault, the orientation and location of the high shear strain coincides roughly with the sECSZ (Fig. 3D).

4. Model sensitivity

As already pointed out, the choice of the boundary conditions for the northern side of the model is not unique and can affect our results, in particular the shear strain rate along the ECSZ. One extreme would be to fix completely the northern model boundary simulating a geological setting where the northern end of the SIERRA block would be part of the NAM plate. This boundary condition would increase the magnitude of shear strain rates in western NAM in the SIERRA driven model, particularly within SIERRA (Fig. 4). In the BAJA driven model, the velocity of SIERRA is lowered significantly, leading to lower shear strain rates across the ECSZ (Fig. 4). However, while the magnitude of the shear strain rate is affected, for both models the presence or absence of significant shear strain gradients and its location do not change significantly by varying the NAM boundary condition in the north. It is also interesting to note that for the BAJA driven fault model, leaving free the northern boundary of the SIERRA block leads to an overestimation of the slip rate accommodated by the nECSZ while fixing the northern boundary led to an underestimation of the slip rate. This is compatible with the fact that in reality the SIERRA block is very well defined on three of its side while the northern termination and fate of the block is not really clear, indicating that this microplate is probably neither completely independent nor completely coupled to NAM.

Our rigid plate velocity boundary conditions imply homogenous mechanical coupling along the PAC plate boundary as a driving force, providing an upper limit of strain concentration at the plate boundaries (e.g. SAF restraining bend). Possible heterogeneities are negligible with respect to the strains associated with the ECSZ formation. We assumed present-day kinematics for BAJA and SIERRA motion following results on constant plate motions since 3 Ma (Dixon et al., 2000b; Plattner et al., 2007) and in absence of better constraints for the past. Lower rates of SIERRA and BAJA motion could be likely due to resisting forces in western NAM and the Protogulf, and in case of the SIERRA driven model, the missing dynamic effect of BAJA on SIERRA motion prior to 6 Ma (Plattner et al., 2009) (Fig. 2). In this case, the shear strain rates could be slightly overestimated. The suggested change in PAC–NAM plate motion azimuth, at 6 Ma from 286° to 305° (Atwater and Stock, 1998; DeMets, 1995) lowers the shear strain in direction of the ECSZ fault strike, but does not affect our conclusions.

Our model geometry is a simplified representation of the western NAM tectonic at 12 to 6 Ma. During this time the Protogulf developed from a weak volcanic arc region into a plate boundary, with unknown mechanical properties. Thus it is important to evaluate the sensitivity of our model results to the presence of this structure. We tested the strain pattern from BAJA and SIERRA driven models in which the Protogulf and the SAF restraining bend do not exist (in this case the rigidity of this volcanic arc region is exaggerated). In the BAJA driven model, BAJA–NAM motion leads to diffuse shear strain south of

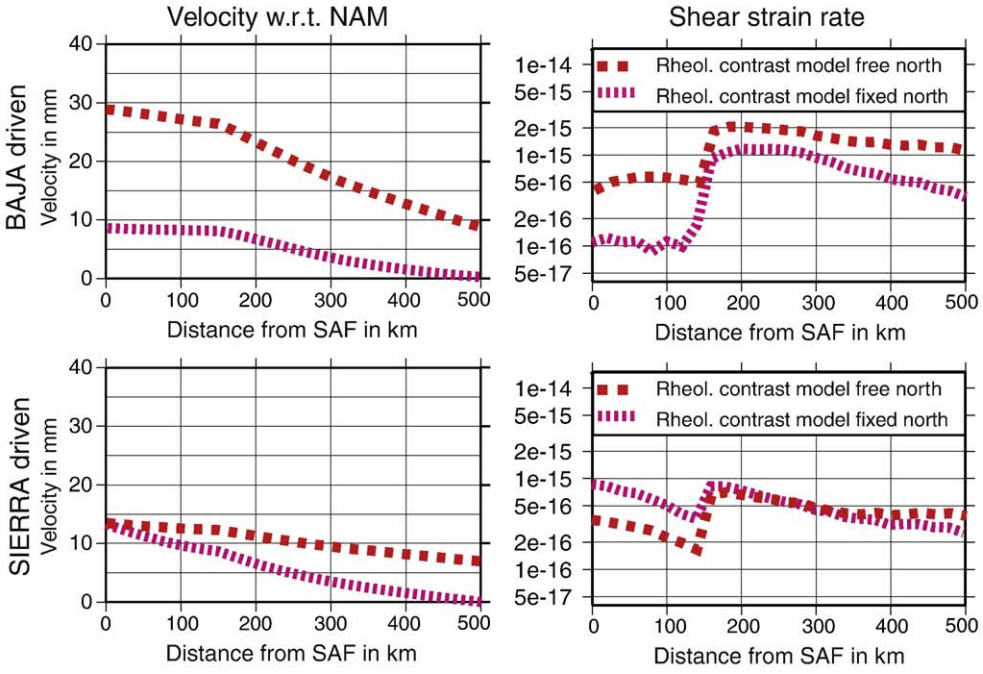

Fig. 4. Influence of northern boundary conditions on the velocity and shear strain rate across the nECSZ (profile A–A′ in Fig. 2), for BAJA driven (upper), and SIERRA driven (lower) models with rheological contrast. Fixing SIERRA and North America in the north decreases the motion of SIERRA in the BAJA driven models. This velocity decrease leads to lower shear strain rates. For the SIERRA driven model the velocity decreases only away from the applied velocity boundary conditions, causing higher shear strain rates within SIERRA. However, in all models shear strain still localizes at the rheological contrast, within the Basin and Range.

latitude 32 N, with the shear pattern resembling the model results for the region along profile A–A′ of the homogenous SIERRA driven model. East of the SIERRA block a pre-existing fault is still activated and accommodates shear strain from BAJA–NAM collision (15–20 mm/year). At the southern termination of this fault a shear-propagation-zone develops (Du and Aydin, 1993), of which the location corresponds to the sECSZ. In a model with rheological weakness, the location of the rheology contrast plays a stronger role for the shear strain pattern in the sECSZ, than in models, in which the Protogulf model fault and the SAF restraining bend model fault exist. Vicinity of the rheological contrast of the sECSZ enhances the shear strain in this region. In the SIERRA driven models, we have seen that the Protogulf model fault, and the SAF restraining bend model fault do not accommodate almost any deformation. This explains why the model results are not sensitive to the presence or abundance of these faults.

The model geometry of the pre-existing weakness is also representative for additional weak structures around the SIERRA such as Pliocene normal faults at the eastern margin of the Sierra Nevada mountain front (Jones et al., 2004). While the fault length, and vicinity to the velocity boundary conditions and regional stress sources such as the SAF restraining bend increase the shear strain accommodation at these structures and shear strain in the sECSZ, multiple parallel faults reduce the shear strain intensity in the sECSZ. Similarly, the vicinity of the rheological contrast to boundary conditions and regional stress sources, as well as the magnitude of the rheological contrast enhances the shear strain accommodated in the weak region.

5. Discussion

McQuarrie and Wernicke (2005) proposed that strike-slip faulting in the nECSZ occurred 12–10 Ma. We tested two end-member models for shear strain in western NAM from motion of the SIERRA, respectively, BAJA mircoplate. The results from our models show that the nECSZ can have evolved at 12–6 Ma by either earlier northward motion of BAJA motion (Fletcher et al., 2007), or driving forces for SIERRA motion, given the pre-existing at the western margin of the Basin and Range.

In all BAJA driven models shear strain is localized at the sECSZ; similar to the results from Li and Liu (2006) we find that the geometrical complexity of the SAF is a key component of this shear zone formation. However, also the accommodation of shear strain from BAJA–NAM collision at a pre-existing weakness (weak Basin and Range or pre-existing faults) in western NAM can have led to localized shear strain in the sECSZ. These results suggest that there is no need for a pre-existing local weakness at the sECSZ, or an intrinsically stronger Mojave block in order to localize strain and initiate the sECSZ. The timing of strike-slip motion at the two parts of the ECSZ depends on the presence of pre-existing weakness. Without any strength heterogeneities in western NAM the nECSZ would form primarily by northward propagation of the sECSZ (Fig. 5A), and thus the nECSZ would be younger than the sECSZ. Conversely, pre-existing weakness in western NAM can be activated to accommodate strain from BAJA–western NAM collision prior to the formation of the sECSZ, beginning with the northward motion of BAJA. It is likely, that between 12 and 6 Ma, BAJA motion occurred at lower rates than today. Thus, BAJA motion became an important driving force for shear strain in western NAM only after 6 Ma, accelerating strike-slip faulting in the nECSZ and driving the shear zone formation at the sECSZ.

In SIERRA driven models, shear strain is only localized at the ECSZ when strength heterogeneities associated with a thermally weakened lithosphere or normal faults in the Basin and Range province pre-exist. These strength heterogeneities allow the SIERRA block to translate without major internal deformation, while shear strain is accommodated adjacent to SIERRA, starting with the beginning

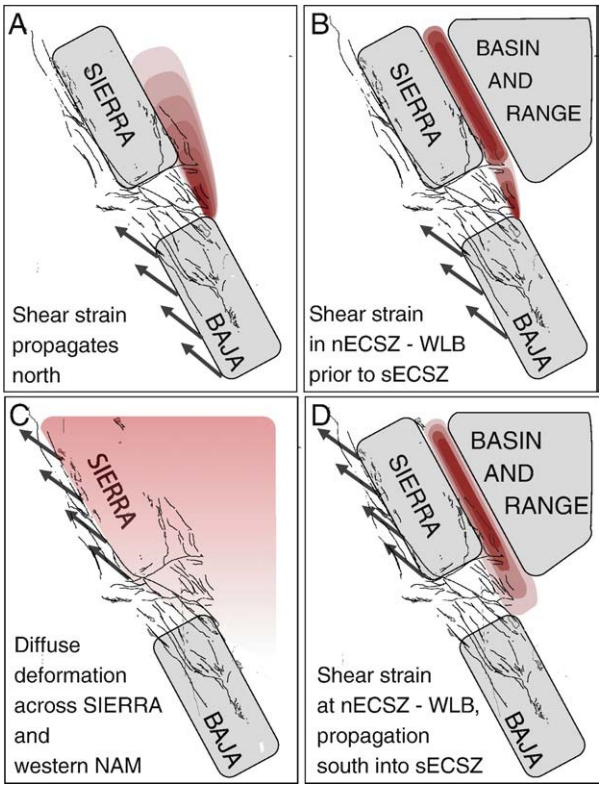

Fig. 5. Schematic illustration of expected location of shear zone development and strain propagation (red color intensity). A) BAJA microplate motion and homogenous strength of western NAM explain the nECSZ by northward migration of shear strain from the sECSZ. B) BAJA microplate motion and strength heterogeneities between SIERRA and Basin and Range allow accommodation of shear strain in nECSZ prior to sECSZ formation. C) Driving forces west of present-day SIERRA cannot explain localized shear strain for a homogenously strong western NAM. Instead of a SIERRA microplate a diffuse deformation zone develops over western NAM. D) Driving forces west of present-day SIERRA microplate lead to high shear strain along nECSZ if strength heterogeneities between SIERRA and Basin and Range are present. The shear zone could even propagate south into sECSZ.

northward motion of this microplate. Thus, northward propagation of the plate boundary in the Gulf of California is not needed to produce the nECSZ (Fig. 5D). Once the shear strain is localized along the nECSZ, the shear zone propagation can even affect the sECSZ (Fig. 5D), High friction along the SAF early after its formation may be an explanation for SIERRA driving forces prior to the beginning of northward motion of BAJA.

Acknowledgements

This research is partially supported by the Deutsche Forschungsgemeinschaft grant MA4163/1-1. C.P. is partially supported by the international graduate school thesis within the Elitenetzwerk Bayern. We want to thank S. Wdowinski and the anonymous reviewer for improving this article, and E. Kirby, P. Umhoefer, and A. Friedrich for helpful discussions.

References

Atwater, T., Stock, J., 1998. Pacific–North America plate tectonics of the Neogene Southwestern United States — an update. In: Ernst, W.G., Nelson, C.A. (Eds.), Integrated Earth and Environmental Evolution of the Southwestern United States: The Clarence A. Hall, Jr. Volume. Bellwether Publishing, Columbia, pp. 393–420.
Bartley, J.M., Glazner, A.F., Schermer, E.R., 1990. North–south contraction of the Mojave block and strike-slip tectonics in southern California. Science 248, 1398–1401.
Beanland, M.M., Clark, 1982. The Owens Valley Fault Zone, eastern California, and surface faulting associated with the 1872 earthquake. U.S. Geol. Surv. Bull. 27 pp.

DeMets, C., 1995. A reappraisal of seafloor spreading lineations in the Gulf of California: implications for the transfer of Baja California to the Pacific plate and estimates of Pacific–North America motion. Geophys. Res. Lett. 22, 3545–3548.
Dixon, T., Farina, F., DeMets, C., Suarez-Vidal, F., Fletcher, J., Marquez-Azua, B., Miller, M., Sanchez, O., Umhoefer, P., 2000a. New kinematic models for Pacific–North America motion from 3 Ma to present, II: evidence for "Baja California shear zone". Geophys. Res. Lett. 27, 3961–3964. doi:10.1029/2000GL008529.
Dixon, T.H., Miller, M., Farina, F., Wang, H., Johnson, D., 2000b. Present-day motion of the Sierra Nevada block and some tectonic implications for the Basin and Range province, North American Cordillera. Tectonics 19 (1), 1–24.
Dokka, R.K., Travis, C.J., 1990. Role of the Eastern California shear zone in accommodating Pacific–North America plate motion. Geophys. Res. Lett. 17 (9), 1323–1326.
Du, Y., Aydin, A., 1993. The maximum distortional strain energy density criterion for shear fracture propagation with applications to the growth paths of en echelon faults. Geophys. Res. Lett. 20, 1091–1094.
Faulds, J.E., Henry, C.D., Hinz, N.H., 2005a. Kinematics of the northern Walker Lane: an incipient transform fault along the Pacific–North American plate boundary. Geology 33 (6), 505–508.
Faulds, J.E., Henry, C.D., Hinz, N.H., Drakos, P.S., Delwiche, B., 2005b. Transect across the Northern Walker Lane, northwest Nevada and northeast California: an incipient transform fault along the Pacific–North America plate boundary. In: Pederson, J., Dehler, C.M. (Eds.), Interior Western United States: Geol. Soc. Am. Field Guide, vol. 6, pp. 129–150. doi:10.1130/2005.fld006(06).
Flesch, L., Holt, W.E., Haines, A.J., Shen-Tu, B., 2000. Dynamics of the Pacific–North American plate boundary in the Western United States. Science 287 (5454), 834–836. doi:10.1126/science.287.5454.834.
Fletcher, J.M., Grove, M., Kimbrough, D., Lovera, O., Gehrels, G.E., 2007. Ridge–trench interactions and the Neogene tectonic evolution of the Magdalena shelf and southern Gulf of California: insights from detrital zircon U–Pb ages from the Magdalena fan and adjacent areas. Geol. Soc. Am. Bull. 199, 1313–1336. doi:10.1130/B26067.1.
Govers, R., Meijer, P.T., 2001. On the dynamics of the Juan de Fuca plate. Earth Planet. Sci. Lett. 189, 115–131. doi:10.1016/S0012-821X(01)00360-0.
Harry, D.L., 2005. Evolution of the western U.S. Walker Lane and East California shear zone: insights from geodynamic modeling. Geol. Soc. Am. Abstract with Programs 37 (7), 59.
Jones, C.H., Farmer, G.L., Unruh, J., 2004. Tectonics of Pliocene removal of lithosphere of the Sierra Nevada, California. Geol. Soc. Am. Bull. 116 (11–12), 1408–1422. doi:10.1130/B25397.1.
Lachenbruch, A.H., Sass, J.H., 1978. Models of an extending lithosphere and heat flow in the Basin and Range Province, in Cenozoic tectonics and regional geophysics of the Western Cordillera. In: Smith, R.S., Eaton, G.P. (Eds.), Geological Society of America Memoir, vol. 152, pp. 209–250. Boulder.
Li, Q., Liu, M., 2006. Geometrical impact of the San Andreas fault on stress and seismicity in California. Geophys. Res. Lett. 33, L08302. doi:10.1029/2005GL025661.
Lonsdale, P., 1991. Structural patterns of the Pacific floor offshore of Peninsular California. In: Dauphin, J.P., Simoneit, B.T. (Eds.), Gulf and Peninsula Province of the Californias: American Association of Petroleum Geologists Memoir, vol. 47, pp. 87–125.
Malservisi, R., Furlong, K.P., Dixon, T.H., 2001. Influence of the earthquake cycle and lithospheric rheology on the dynamics of the Eastern California shear zone. Geophys. Res. Lett. 28 (14), 2731–2734. doi:10.1029/2001GL013311.
McCrory, P.A., Wilson, D.S., Stanley, R.G., 2009. Continuing evolution of the Pacific–Juan de Fuca–North America slab window system — a trench–ridge-transform example from the Pacific Rim. Tectonophysics 464, 30–42. doi:10.1016/j.tecto.2008.01.018.
McQuarrie, N., Wernicke, B.P., 2005. An animated tectonic reconstruction of southwestern North America since 36 Ma. Geosphere 1 (3), 147–172.
Meade, B.J., 2007. Power-law distribution of fault slip-rates in southern California. Geophys. Res. Lett. 34, L23307. doi:10.1029/2007GL031454.
Melosh, H.J., William, C.A., 1989. Mechanics of graben formation in crustal rocks — a finite-element analysis. J. Geophys. Res. 94, 13,961–13,973. doi:10.1029/JB094iB10p13961.
Miller, D.M., Yount, J.C., 2002. Late Cenozoic tectonic evolution of the north-central Mojave Desert inferred from fault history and physiographic evolution of the Fort Irwin area, California. In: Glazner, A.F., Walker, J.D., Bartley, J.M. (Eds.), Geologic Evolution of the Mojave Desert and Southwestern Basin and Range. Geological Society of America Memoir, vol. 195. Geological Society of America, Boulder, CO, pp. 173–197.
Miller, M.M., Johnson, D.J., Dixon, T.H., Dokka, R.K., 2001. Refined kinematics of the Eastern California shear zone from GPS observations, 1993–1998. J. Geophys. Res. 106 (B2), 2245–2263.
Monastero, F.C., Sabin, A.E., Walker, J.D., 1997. Evidence for post–early Miocene initiation of movement on the Garlock fault from offset of the Cudahy Camp Formation, east-central California. Geology 25, 247–250. doi:10.1130/0091-7613(1997)025.
Nicholson, C., Sorlien, C.C., Atwater, T., Crowell, J.C., Luyendyk, B.P., 1994. Microplate capture, rotation of the Western Transverse Ranges, and initiation of the San Andreas transform as a low-angle fault system. Geology 22, 491–495. doi:10.1130/0091-7613(1994)022<0491:MCROTW>2.3.CO;2.
Oskin, M., Iriondo, A., 2004. Large-magnitude transient strain accumulation on the Blackwater fault. Eastern California shear zone, Geology 32, 313–316. doi:10.1130/G20223.1.
Plattner, C., Malservisi, R., Dixon, T.H., LaFemina, P., Sella, G.F., Fletcher, J., Suarez-Vidal, F., 2007. New constraints on relative motion between the Pacific Plate and Baja California microplate (Mexico) from GPS measurements. Geophys. J. Int. 107 (3), 1373–1380. doi:10.1111/j.1365-246X.2007.03494.x.
Plattner, C., Malservisi, R., Govers, R., 2009. On the plate boundary forces that drive and resist Baja California motion. Geology 37, 359–362. doi:10.1130/G25360A.1.
Psencik, K.O., Dixon, T.H., Schmalzle, G., McQuarrie, N., McCaffrey, R., 2006. Improved Present Day Euler Vector for Sierra Nevada Block Using GPS. EOS (trans. Am. Geophys. Un.), Fall Meeting Supplement, Abstract G42A-04.
Ranalli, G., 1995. Rheology of the Earth2nd ed. Chapman and Hall, London. 413 pp.
Reheis, M.C., Sawyer, T.L., 1997. Late Cenozoic history and slip rate of Fish Lake Valley, Emigrant Peak, and Deep Springs fault zones, Nevada and California. Geol. Soc. Am. Bull. 109 (3), 280–299.
Sandwell, D., Sichox, L., Agnew, D., Bock, Y., Minster, J.-B., 2000. Near real-time radar interferometry of the Mw 7.1 Hector Mine Earthquake. Geophys. Res. Lett. 27 (9), 3101–3104.
Stock, J.M., Hodges, K.V., 1989. Pre-Pliocene extension around the Gulf of California and the transfer of Baja California to the Pacific Plate. Tectonics 8 (1), 99–115.